Inorganic Chemistry

Article

pubs.acs.org/IC

Exploring Cyclometalated Ir Complexes as Donor Materials for Organic Solar Cells

Tyler B. Fleetham, Zixing Wang, and Jian Li*

Material Science and Engineering, Arizona State University, Tempe, Arizona 85287, United States

Supporting Information

ABSTRACT: The performance of small molecular organic photovoltaic materials is typically limited by their low exciton diffusion lengths, poor solubility, and poor energy level alignment with fullerenes so that the design and synthesis of new materials remain a top priority. To overcome these limitations, we explored the use of an iridium complex as a donor material with the potential for compatibility with solution processing, long exciton diffusion length and easy molecular modification for tunable optical or electrical properties. A bilayer device with a cyclometalated iridium complex and C_{60} resulted in a power conversion efficiency as high as 2.8%. Furthermore, a V_{OC} of 1 V was achieved in the bilayer device despite an estimated exciton energy of only 1.55 eV, and the device showed minimal temperature and light intensity dependence.

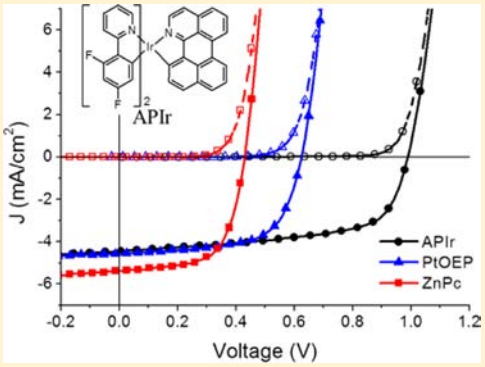

INTRODUCTION

Recently, organic photovoltaics (OPVs) have gained significant attention due to their potential as a cost-effective alternative to existing photovoltaic (PV) technology which focuses on inorganic semiconductors in crystalline or polycrystalline forms.[1,2] The fabrication cost of OPVs can be significantly reduced with the use of plastic substrates[3] and well-established printing techniques in a roll-to-roll process.[4] However, the power conversion efficiency (η_p) of the best organic solar cells is around 10%,[5] which is still much lower than that of inorganic PVs (~30%).[6] Thus, the materials development for organic PVs remains as a top priority.

Although cyclometalated Ir and Pt complexes are under heavy investigation as phosphorescent emitters for organic light-emitting diodes (OLEDs),[7] the success of these metal complexes in OPVs has been limited.[8,9] This can be attributed to the fact that currently available metal complexes do not absorb strongly in the red and near-infrared (NIR) region since they were designed for full color displays with maximum emission wavelengths in the range of 450−650 nm.[7] Moreover, metal complexes with ligands absorbing strongly and broadly in the visible and NIR ranges tend to have more complex molecular structures, making the process of materials synthesis and purification more difficult. However, the past studies focusing on the cyclometalated metal complexes for OLED applications indicated that this class of materials can have favorable photophysical and electrochemical stability,[10] versatility in the modification of molecular properties,[11] tunable highest occupied molecular orbital (HOMO) and lowest unoccupied molecular orbital (LUMO),[12] long exciton lifetime,[13] and potentially long exciton diffusion length.[14] These properties make a compelling case that cyclometalated metal complexes can be an excellent material candidate for PV applications with a judicious material design. In this short communication, we will demonstrate that metal complexes, and in particular, a selected Ir complex, can be used as a donor-type material to fabricate an efficient organic solar cell.

RESULTS AND DISCUSSION

In order to develop Ir complexes as absorbers for organic PVs, ligands with strong absorption are needed. Thus, azaperylene[15] (AP) was chosen as a cyclometalating ligand to Ir complexes due to its structural similarity to commonly used organic dyes such as PTCDA and other perylene-based OPV materials.[16−18] The ligand of difluoro-phenyl-pyridine (dfppy) was chosen to increase oxidation potential (i.e., lower the HOMO energy level) and improve the volatility (i.e., lower the sublimation temperature) of the proposed metal complex.[19,20] The synthetic process of mer-bis(4′,6′-difluorophenylpyridinato-N,C_2') iridium(III) azaperylene (denoted APIr) is shown in Scheme 1. The reaction between the chloride-bridged Ir(III) dimer, $[(dfppy)_2Ir(\mu\text{-}Cl)]_2$, and the ligand readily yields the product with the assistance of silver triflate and excess base in a refluxed solution of dichloroethane.

The absorption spectra of APIr and the corresponding AP ligand in solution are shown in Figure 1. Both AP and APIr are observed to have high energy and intense absorption bands (380−460 nm, $\varepsilon > 10^4$ cm^{-1} M^{-1}) similar to those of perylene.[21] Moreover, the cyclometalation results in lower energy and intense absorption bands (460−560 nm, ε = 6000−8000 cm^{-1} M^{-1}) due to the newly formed Ir→AP transitions. The weak, lowest energy absorption band (782 nm, ε = 30 cm^{-1} M^{-1}) can be identified as a triplet absorption on the basis

Received: October 26, 2012
Published: June 17, 2013

   dx.doi.org/10.1021/ic3023453 | Inorg. Chem. 2013, 52, 7338−7343

Scheme 1. Synthetic Conditions for APIr

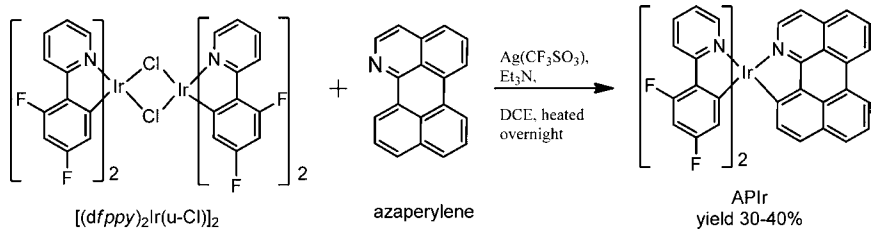

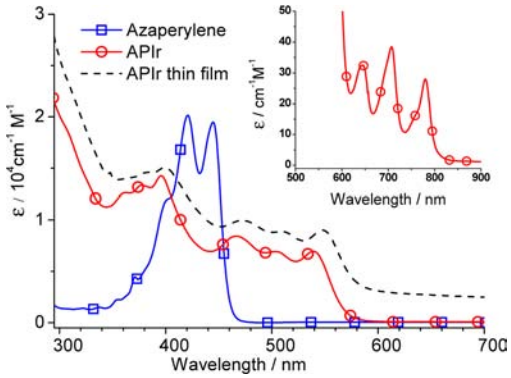

Figure 1. The absorption spectra of azaperylene (squares) and APIr (circles) in a solution of dichloromethane. The thin film absorption spectrum of APIr (dotted lines) is scaled for comparison to solution spectrum. (Inset) Triplet absorption of APIr in dichloromethane is shown.

of the small Stokes shift between absorption (Figure 1 inset) and emission (Figure 2) at the room temperature. It is

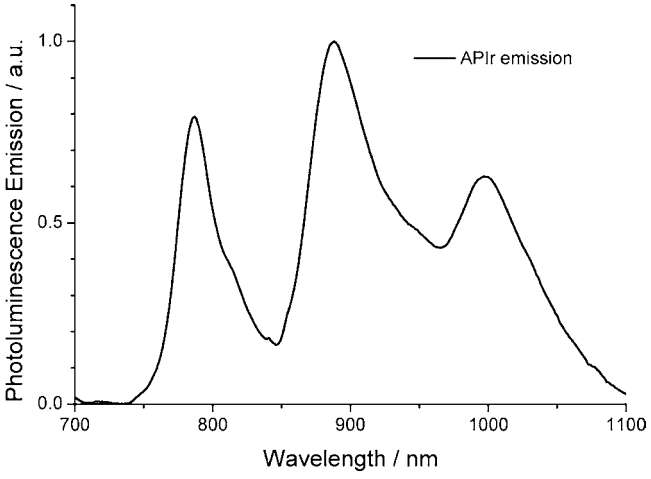

Figure 2. The emission spectrum of APIr in a solution of dichloromethane.

noteworthy that the intensities of both ligand-centered (LC) and metal-to-ligand-charge-transfer (MLCT) transitions of APIr are higher than the rest of reported $(dfppy)_2Ir$-based complexes,[19,20] indicating that the incorporation of a ligand like AP makes Ir complexes better suited as absorber materials. The thin film absorption spectrum of APIr in Figure 1 shows that there is a minimal change in the absorption features upon depositing in a thin film, suggesting minimal stacking or intermolecular interaction for APIr molecules in the amorphous film.

The electrochemical properties of APIr and AP were examined using cyclic voltammetry, and the values of redox potentials were determined using differential pulsed voltammetry. All of the electrochemical data reported here were measured relative to an internal ferrocenium/ferrocene reference (Fc^+/Fc). The oxidation and reduction values for APIr are 0.56 V and −1.87 V, while those for AP are 0.46 V and −1.90 V. The similarity in the oxidation values between APIr and other commonly used donor-type absorbers like metal phthalocyanines makes APIr suitable as a donor material for PV applications.[22] Moreover, it is also worth noting that APIr has a higher oxidation potential than the corresponding cyclometalating ligand (AP), which is not very common for such class of materials.[7c] This can be attributed to the use of the dfppy ligand which lowers the electron density of metal ions and makes the complex more difficult to oxidize.[19,20]

APIr and azaperylene were first evaluated in a bilayer solar cell device with a general structure of ITO/donor (5 nm)/ C_{60} (30 nm)/PTCDI (10 nm)/BCP (14 nm)/Al. *N,N′*-Dihexyl-perylene-3,4,9,10-bis(dicarboximide) (PTCDI) was added as an interfacial layer between the C_{60} acceptor layer and the bathocuproine (BCP) exciton blocking layer to improve the electron injection.[23] For comparison, control devices were fabricated simultaneously with zinc phthalocyanine (ZnPc) or Pt(II) octaethylporphine (PtOEP) as donor materials. The current density versus voltage ($J-V$) characteristics measured under both dark and 1 sun AM1.5G simulated illumination are shown in Figure 3.

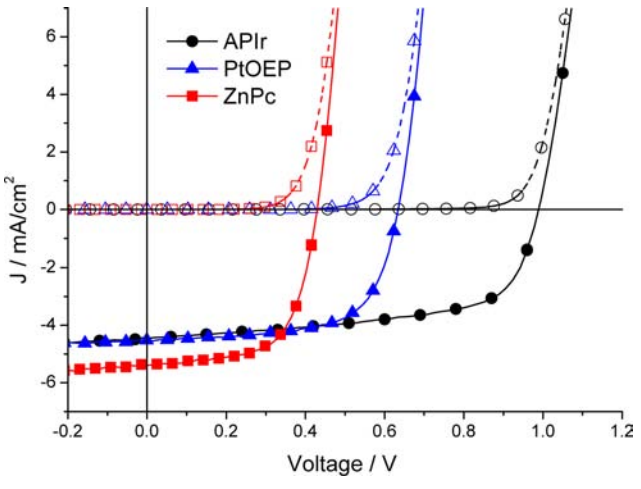

Figure 3. Current−voltage characteristics of APIr (circles), PtOEP (triangles)- and ZnPc (squares)-based bilayer solar cells under dark (open) and 1sun AM 1.5 G simulated illumination (solid) in the device architecture ITO/donor (5 nm)/ C_{60} (30 nm)/PTCDI (10 nm)/BCP (14 nm)/Al.

dx.doi.org/10.1021/ic3023453 | *Inorg. Chem.* 2013, 52, 7338−7343

The reasonable photocurrent and diode behavior demonstrate that select cyclometalated Ir complexes like APIr can function as donor-type materials in a bilayer device with C_{60} as an acceptor-type material. On the other hand, azaperylene cannot form a stable amorphous film, resulting in a device failure in a similar device structure. Moreover, the APIr device has J_{SC} of 4.5 mA/cm^2, FF of 0.62, and V_{OC} of 0.99 V, leading to a high η_P of nearly 2.8% which is noteworthy for a simple bilayer device employing only a 5 nm donor layer. In comparison, PtOEP- and ZnPc- based devices had J_{SC} of 4.6 mA/cm^2 and 5.4 mA/cm^2, FF of 0.64 and 0.63, V_{OC} of 0.62 and 0.43 V, and η_P of 1.8% and 1.5%, which are comparable to the literature reports on the same materials.[24,25] Compared with APIr- and PtOEP-based devices, ZnPc device generates more photocurrent, which can be attributed to its enhanced response (stronger absorption) in the range of 600−800 nm.

In order to fully utilize the benefits of APIr, enhancing J_{SC} is necessary to achieve. To realize improvement in J_{SC} through increasing active layer thicknesses, long exciton diffusion lengths are necessary. Previous reports suggest that phosphorescent materials such as APIr may have a longer exciton diffusion length due to their strong triplet character.[13] Thus, the exciton diffusion lengths for both APIr and PtOEP were determined using photoluminescent (PL) quenching calculations.[26] The exciton diffusion length for ZnPc, however, could not be determined using this method due to significant self-absorption but has been previously estimated at 5 nm.[25] Thin films of PtOEP and APIr with various donor layer thicknesses with and without a C_{60} quenching layer were deposited. The exciton diffusion efficiency, η_{ED}, is plotted against donor layer thickness in Figure 4, from which the exciton diffusion length is

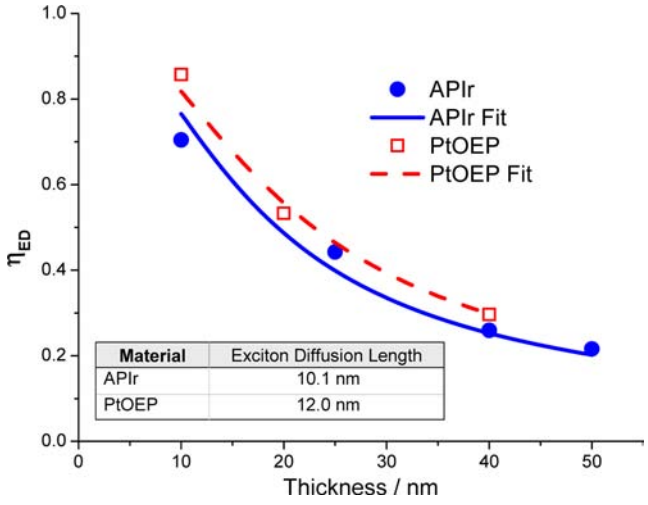

Figure 4. Plots of exciton diffusion efficiency (η_{ED}) vs the film thickness for APIr (circles) and PtOEP (squares) materials. The derived exciton diffusion lengths (L_D) of APIr and PtOEP are shown in the inset of the figure.

determined (Figure 4 Inset). The estimated exciton diffusion length for both APIr and PtOEP are greater than 10 nm which is much higher than that of phthalocyanine materials such as ZnPc. Therefore, it would be expected that creating thicker films of these phosphorescent donor materials would yield higher current densities.

To determine the effect of donor layer thickness, devices were fabricated with donor thicknesses from 5 to 20 nm, current−voltage characteristics are given in Figures S1−S3 in Supporting Information (SI). The device performance parameters given in Figure 5 showed small changes in V_{OC} for all three donor materials. Also, the devices for both PtOEP and ZnPc showed minimal changes in J_{SC}, yet the devices for APIr decreased significantly from 5 to 20 nm. Additionally, the APIr device demonstrated a more pronounced drop in FF compared to those of ZnPc and PtOEP devices. These trends are likely due to the minimal stacking of the octahedral APIr molecules, resulting in reduced intermolecular orbital overlap leading to a slower charge-hopping process and a lower mobility. Thus, the benefits of long exciton diffusion length and large V_{OC} could not be fully utilized due to the restriction on APIr thickness.

The high η_P value of the APIr device compared with ZnPc and PtOEP can be mainly attributed to its large V_{OC} despite their similar oxidation values.[24,25] The HOMO and LUMO energy levels of APIr and AP, as well as those of ZnPc and PtOEP, are provided in the inset of Figure 6, based on estimation from the oxidation and reduction values.[27] The achievement of 0.99 V V_{OC} is among the highest reported values for bilayer small-molecule OPVs, and this boost in V_{OC} is a significant step in the formation of future high-efficiency OPVs. Moreover, it is encouraging that a large V_{OC} (1.0 V) can be generated despite an exciton energy of only about 1.55 eV (based on the emission spectrum of APIr, Figure 2). Uncovering factors resulting in this high V_{OC} is critical to the goal of maximizing the device efficiency of organic solar cells and minimizing unnecessary power loss due to low V_{OC}.

The difference in V_{OC} among ZnPc, PtOEP, and APIr is attributed to a decrease in the dark (diode) current due in part to an increase in the donor−acceptor energy offset from the change in APIr HOMO level.[28] However, a 0.2 eV reduction in APIr HOMO level does not fully explain such a dramatic increase in V_{OC}. Previous reports suggest that the V_{OC} is strongly related to the molecular geometry of the donor materials.[29] Thus, the increase in V_{OC} may be influenced by adopting an octahedral geometry compared the planar structures of the porphyrin and phthalocyanine donors. To further explore the effect of the donor material on V_{OC} the devices were tested at various illumination intensities using neutral density filters and at various temperatures using a liquid nitrogen-cooled cryostat (Janis VNF100) for a temperature range from 100 K to room temperature. Previously reported experiments have shown that V_{OC} approaches a maximum attainable value at low temperatures and maximum light intensities.[30] Thus, under typical operating conditions of 1 sun and room temperature the V_{OC} could be significantly lower than the maximum attainable value. Consequently, in order to avoid the costly and complex operation at high light intensities and low temperatures, devices and materials should be designed to give as close to the maximum attainable value of V_{OC} as possible under typical operation conditions of 1 sun and room temperature. It is evident from the temperature dependencies given in Figure 6 that both ZnPc and PtOEP show this behavior of enhanced V_{OC} at low temperatures approaching a maximum value at 150 K and high light intensities. These two materials also show continual increases in V_{OC} for illumination intensities up to 3 suns shown in Figure 7. The V_{OC} of APIr, however, is almost independent of the temperature change and shows minimal improvement in V_{OC} at illumination intensities beyond 1 sun. As a result, the V_{OC} at 1 sun and room temperature is well over 90% of its maximum attainable value. The reason for the different temperature dependencies of the

dx.doi.org/10.1021/ic3023453 | Inorg. Chem. 2013, 52, 7338−7343

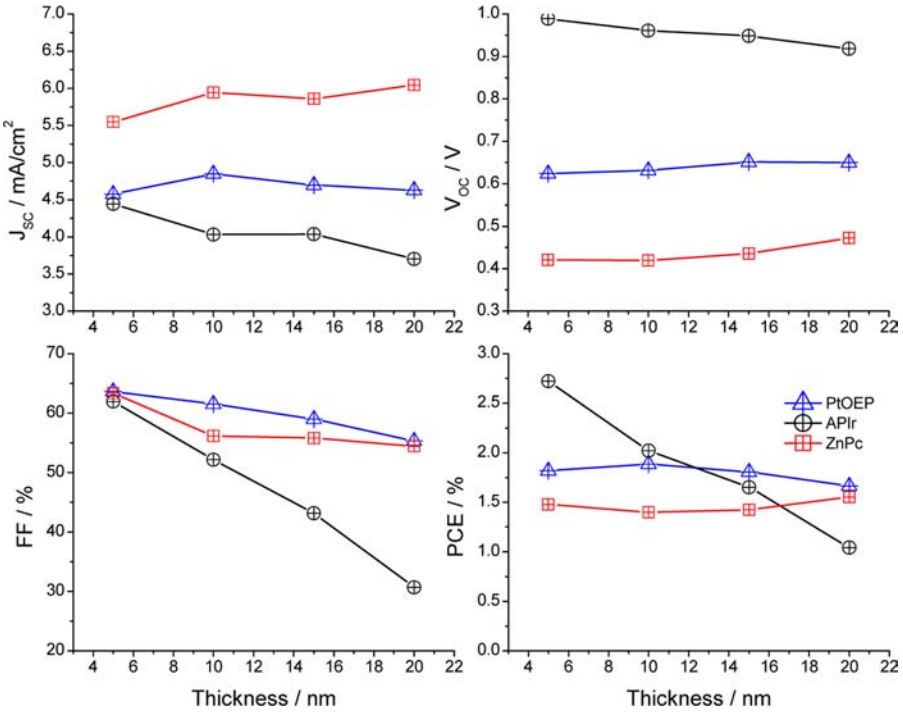

Figure 5. Dependence of device characteristics of APIr (circles)-, PtOEP (triangles)-, and ZnPc (squares)-based bilayer solar cells on the thickness of donor layer with a general structure of ITO/donor (x nm)/C_{60} (30 nm)/PTCDI (10 nm)/BCP (14 nm)/Al. The data are reported under AM1.5G 1 sun conditions.

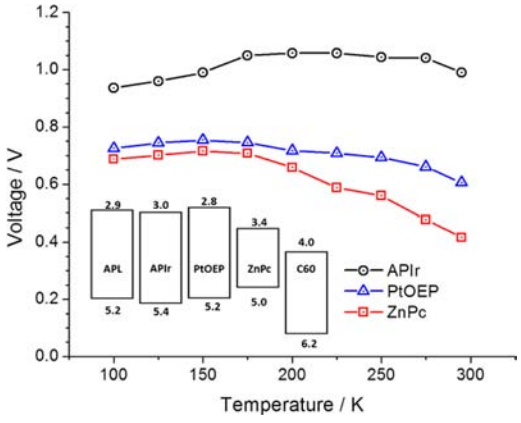

Figure 6. Temperature dependence of V_{OC} for APIr (circles), PtOEP (triangles), and ZnPc (squares) in the device architecture ITO/donor (5 nm)/C_{60} (30 nm)/PTCDI (10 nm)/BCP (14 nm)/Al.

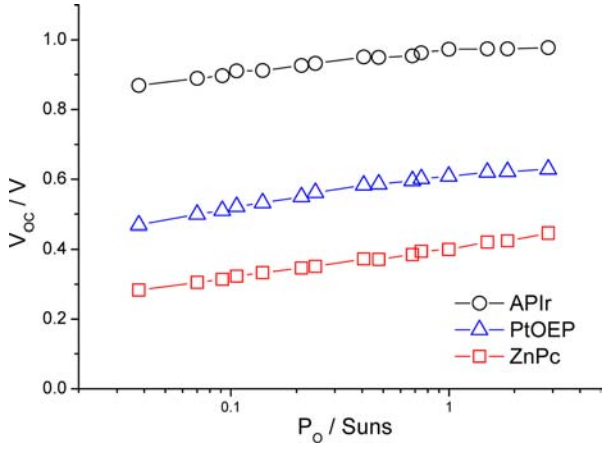

Figure 7. Plots of V_{oc} vs illumination intensity for APIr (circles), PtOEP (triangles), and ZnPc (squares) devices, with a general structure of ITO/donor (5 nm)/C_{60} (30 nm)/PTCDI (10 nm)/BCP (14 nm)/Al.

V_{OC} for the different donor materials is under continued investigation.

CONCLUSIONS

In conclusion, cyclometalated Ir complexes have been demonstrated to work efficiently as absorbers for solar cell applications. An efficient bilayer organic PV cell with η_p of 2.8% was fabricated with APIr as a donor-type material. Compared with its organic counterpart, Ir complexes can have improved thermal stability, broader absorption spectrum, and tunable HOMO and LUMO energy levels. In addition, compared to commonly used porphyrin complexes, APIr showed dramatically improved V_{OC} despite having similar oxidation and reduction potentials. Furthermore, the high V_{OC} of APIr devices showed minimal temperature and light intensity dependence. As a result, nearly 1 V V_{OC} was achieved at typical operating conditions for an absorber material with an approximated exciton energy of only 1.55 eV. Future development of Ir complexes with improved mobility and wider absorption range will enable this class of materials to make an even more significant impact.

EXPERIMENTAL SECTION

Synthesis: General Procedures. The UV−visible spectra were recorded on a Cary 5G UV−vis−NIR spectrometer (Varian). Steady-state emission experiments at room temperature were performed on a Horiba Jobin Yvon FluoroLog-3 spectrometer. NMR spectra were recorded on a Varian Gemini-300 MHz spectrometer with $Si(CH_3)_4$ as the internal reference, and chemical shifts were referenced to residual

dx.doi.org/10.1021/ic3023453 | Inorg. Chem. 2013, 52, 7338−7343

protiated solvent. The Microanalysis Laboratory at the University of Illinois, Urbana−Champaign, performed the elemental analysis.

The Synthesis of Mer-bis(4′,6′-difluorophenylpyridinato-N,C$_2$′) iridium(III) Azaperylene (APIr). A mixture of chloride-bridged Ir(III) dimer $[(dfppy)_2Ir(\mu\text{-}Cl)]_2$ (0.3 g, 0.25 mmol), azaperylene ligand (0.15 g, 0.24 mmol), silver triflate (0.3 g, 1.17 mmol), and 2−3 equiv of triethylamine was stirred in a solution of 50 mL dichloroethane for 2 h at room temperature. The reaction mixture was heated to reflux for additional 12 h. Then the mixture was cooled to room temperature, and the precipitate was filtered off. The filtrate was evaporated to dryness under reduced pressure, and the dark red crystalline product (yield 40%) was obtained from column chromatography on silica using a CH_2Cl_2 mobile phase. The final product can be further purified in a thermal gradient sublimation method. The ^{1}H NMR spectrum of the resulting product is given in Figure S4b in the SI. ^{1}H NMR (300 MHz, $CDCl_3$), 8.31 (d, J = 7.8 Hz, 1H), 8.27−8.15 (m, 3H), 7.97 (d, J = 5.3 Hz 1H), 7.75−7.64 (m, 3H), 7.59−7.41 (m, 6H), 7.28 (d, J = 8.4 Hz,1H), 7.14 (d, J = 5.7 Hz,1H), 6.69 (dd, J = 6.0 Hz, 6.6 Hz, 1H), 6.65(dd, J = 6.6 Hz, 6.6 Hz, 1H), 6.52−6.41 (m, 2H), 6.06(dd, J = 7.5 Hz, J = 2.4 Hz, 1H), 5.93 (dd, J = 8.4 Hz, J = 2.4 Hz, 1H). Anal. for $C_{41}H_{22}F_4IrN_3$, found: C 59.83, H 2.36, N 5.11; calcd: C 59.70, H 2.69, N 5.09.

Electrochemistry. Cyclic voltammetry and differential pulsed voltammetry were performed to determine electrochemical properties using a CHI610B electrochemical analyzer. Pure samples were dissolved in anhydrous DMF (Aldrich) under a nitrogen atmosphere with a 0.1 M tetra(n-butyl)ammonium hexafluorophosphate supporting electrolyte. A silver wire was used as the pseudo reference electrode, a platinum wire was used as the counter electrode, and glassy carbon was used as the working electrode. The redox potentials are based on the values measured from differential pulsed voltammetry and are reported relative to a ferrocene/ferrocenium (Fc/Fc^+) redox couple used as an internal reference. The reversibility of reduction or oxidation was determined using cyclic voltammetry.

Exciton Diffusion Length Measurement. The photoluminescent (PL) signals from thin films of a donor material of a known thickness and fixed position were measured using a Horiba Jobin Yvon FluoroLog-3 spectrometer. The exciton diffusion efficiency for a given thickness was determined from the following equation: $\eta_{ED} = 1 - PL_1/PL_2$, where PL_1 is the PL signal for the donor material thin film deposited on top of a C_{60} quenching interface and PL_2 is the signal without the C_{60} quenching interface. Exciton diffusion lengths were then determined by fitting the exciton diffusion efficiency versus thickness data to the following equation as reported in previous literature:[1]

$$\eta_{ED} = \frac{L_D}{d}\frac{[1 - \exp(-2d/L_D)]}{[1 + \exp(-2d/L_D)]}$$

where L_D is the exciton diffusion length, d is the film thickness, and η_{ED} is the exciton diffusion efficiency.

Device Fabrication and Characterization. OPV devices were fabricated on glass substrates precoated with a patterned transparent indium tin oxide (ITO) anode. Prior to organic depositions the ITO substrates were cleaned by sonication in water, acetone, and isopropanol followed by a 15 min UV−ozone treatment. Organic materials were deposited by high-vacuum thermal evaporation at a base pressure ~1×10^{-7} Torr. The film thickness was monitored by quartz crystal microbalances, and typical deposition rates of the organic thin films are in the range of 0.5−1.5 Å/s and 1−2 Å/s for the Al cathode. The ITO and Al electrodes were patterned to form device areas of 4 mm^2 in cross-bar geometry. Zinc phthalocyanine (ZnPc) and bathocuproine (BCP) were purchased from Sigma Aldrich, C_{60} was purchased from MER Corporation, Pt(II) octaethylporphine (PtOEP) was purchased from Porphyrin Products Inc., and N,N'-dihexyl-perylene-3,4,9,10-bis(dicarboximide) (PTCDI) was synthesized following the previous literature report.[24] All organic materials synthesized or purchased were purified using the thermal gradient sublimation method prior to use.

Current−voltage (I−V) characteristics in the dark and under illumination were measured using a Keithley 2400 source meter in a nitrogen-filled glovebox. Illumination was provided by a Newport 150-W Xe-arc solar simulator outfitted with an AM1.5G filter and neutral density filters provided 1 sun light intensity determined using a Hamamatsu Si reference cell (model C24 S1787-04) calibrated by NREL. The spectral mismatch is estimated to be less than 10%. For tests of variable-light intensities, neutral density filters were used. For variable-temperature testing, a Janis VNF100 series liquid nitrogen-cooled cryostat was used to control the temperature from 100 to 300 K while the incident light was kept at the elevated intensity of approximately 2 suns.

■ ASSOCIATED CONTENT

Ⓢ Supporting Information

The NMR spectrum of the synthesized metal complex, APIr. The current−voltage characteristics for APIr, PtOEP, and ZnPc for various donor layer thicknesses between 5 nm and 20 nm. This material is available free of charge via the Internet at http://pubs.acs.org.

■ AUTHOR INFORMATION

Corresponding Author

*E-mail: Jian.Li.1@asu.edu.

Notes

The authors declare no competing financial interest.

■ ACKNOWLEDGMENTS

We thank the National Science Foundation under award numbers CHE-0748867 and OISE-1210250, and Advanced Photovoltaics Center for partial support of this work.

■ REFERENCES

(1) Peumans, P.; Yakimov, A.; Forrest, S. R. *J. Appl. Phys.* **2003**, *93*, 3693.
(2) Mishra, A.; Bäuerle, P. *Angew. Chem., Int. Ed.* **2012**, *51*, 2020.
(3) Forrest, S. R. *Nature* **2004**, *428*, 911.
(4) Krebs, F. C. *Org. Electron.* **2009**, *10*, 761.
(5) He, Z.; Zhong, C.; Su, S.; Xu, M.; Wu, H.; Cao, Y. *Nat. Photon.* **2012**, *6*, 591.
(6) Green, M. A.; Emery, K.; Hishikawa, Y.; Warta, W.; Dunlop, E. D. *Prog. Photovolt.: Res. Appl.* **2012**, *20*, 12.
(7) (a) Fleetham, T.; Wang, Z.; Li, J. *Org. Electron.* **2012**, *13*, 1430. (b) Vezzu, D. A. K.; Deaton, J. C.; Jones, J. S.; Bartolotti, L.; Harris, C. F.; Marchetti, A. P.; Kondakova, M.; Pike, R. D.; Huo, S. *Inorg. Chem.* **2010**, *49*, 5107. (c) Lamansky, S.; Djurovich, P.; Murphy, D.; Abdel-Razzaq, F.; Lee, H.-E.; Adachi, C.; Burrows, P. E.; Forrest, S. R.; Thompson, M. E. *J. Am. Chem. Soc.* **2001**, *123*, 4304. (d) Wong, W.-Y.; Ho, C.-L. *J. Mater. Chem.* **2009**, *19*, 4457. (e) Zhou, G.; Wang, Q.; Ho, C.-L.; Wong, W.-Y.; Ma, D.; Wang, L. *Chem. Commun.* **2009**, 3574. (f) Zhou, G.; Wang, Q.; Wang, X.; Ho, C.-L.; Wong, W.; Ma, D.; Wang, L.; Lin, Z. *J. Mater. Chem.* **2010**, *20*, 7472.
(8) (a) Wong, W. Y.; Ho, C. L. *Acc. Chem. Res.* **2010**, *43*, 1246. (b) Wong, W.-Y.; Wang, X.-Z.; He, Z.; Djurisic, A. B.; Yip, C.-T.; Cheung, K.-Y.; Wang, H.; Mak, C. S. K.; Chan, W.-K. *Nat. Mater.* **2007**, *6*, 521. (c) Liu, L.; Ho, C.-L.; Wong, W.-Y.; Cheung, K.-Y.; Fung, M.-K.; Lam, W.-T.; Djurisici, A. B.; Chan, W.-K. *Adv. Funct. Mater.* **2008**, *18*, 2824.
(9) (a) Lee, W.; Kwon, T.-H.; Kwon, J.; Kim, J.-K.; Lee, C.; Hong, J.-I. *New J. Chem.* **2011**, *35*, 2557. (b) Huang, J.; Yu, J.; Guan, Z.; Jiang, Y. *Appl. Phys. Lett.* **2010**, *97*, 143301. (c) Yu, J.; Zang, Y.; Li, H.; Huang, J. *Thin Solid Films* **2012**, *520*, 6653.
(10) Tamayo, A. B.; Alleyne, B. D.; Djurovich, P. I.; Lamansky, S.; Tsyba, I.; Ho, N. N.; Bau, R.; Thompson, M. E. *J. Am. Chem. Soc.* **2003**, *125*, 7337.

(11) Wang, Z.; Turner, E.; Mahoney, V.; Madakuni, S.; Groy, T.; Li. *J. Inorg. Chem.* **2010**, *49*, 11276.
(12) Yang, C. L.; Zhang, X. W.; You, H.; Zhu, L. Y.; Chen, L. Q.; Zhu, L. N.; Tao, Y. T.; Ma, D. G.; Shuai, Z. G.; Qin, J. G. *Adv. Funct. Mater.* **2007**, *17*, 651.
(13) Baldo, M. A.; O'Brien, D. F.; You, Y.; Shoustikov, A.; Sibley, S.; Thompson, M. E.; Forrest, S. R. *Nature* **1998**, *395*, 151.
(14) Baldo, M. A.; O'Brien, D. F.; Thompson, M. E.; Forrest, S. R. *Phys. Rev. B* **1999**, *66*, 14422.
(15) Gryko, D. T.; Piechowska, J.; Galzeowski, M. *J. Org. Chem.* **2010**, *75*, 1297.
(16) Tang, C. W. *Appl. Phys. Lett.* **1986**, *48*, 183.
(17) Kim, I.; Haverinen, H. M.; Wang, Z.; Madakuni, S.; Li, J.; Jabbour, G. E. *Appl. Phys. Lett.* **2009**, *95*, 023305.
(18) Wagner, J.; Gruber, M.; Hinderhofer, A.; Wilke, A.; Bröker, B.; Frisch, J.; Amsalem, P.; Vollmer, A.; Opitz, A.; Koch, N.; Frank, S.; Brütting, W. *Adv. Funct. Mater.* **2010**, *20*, 4295.
(19) Li, J.; Djurovich, P. I.; Alleyne, B. D.; Yousufuddin, M.; Ho, N. N.; Thomas, J. C.; Peters, J. C.; Bau, R.; Thompson, M. E. *Inorg. Chem.* **2005**, *44*, 1713.
(20) Brooks, J.; Babayan, Y.; Lamansky, S.; Djurovich, P. I.; Tsybe, I.; Bau, R.; Thompson, M. E. *Inorg. Chem.* **2002**, *41*, 3055.
(21) Quante, H.; Geerts, Y.; Müllen, K. *Chem. Mater.* **1997**, *9*, 495.
(22) Bruder, I.; Schöneboom, J.; Dinnebier, R.; Ojala, A.; Schaäfer, S.; Sens, R.; Erk, P.; Weiss, J. *Org. Elect.* **2010**, *11*, 377.
(23) Kim, I.; Haverinen, H. M.; Li, J.; Jabbour, G. E. *Appl. Mater. Interfaces* **2010**, *2*, 1390.
(24) Shao, Y.; Yang, Y. *Adv. Mater.* **2005**, *17*, 2841.
(25) Kim, I.; Haverinen, H. M.; Wang, Z.; Madakuni, S.; Kim, Y.; Li, J.; Jabbour, G. E. *Chem. Mater.* **2009**, *21*, 4256.
(26) Lunt, R. R.; Giebink, N. C.; Belak, A. A.; Benziger, J. B.; Forrest, S. R. *J. Appl. Phys.* **2009**, *105*, 053711.
(27) D'andrade, B. W.; Datta, S.; Forrest, S. R.; Djurovich, P.; Polikarpov, E.; Thompson, M. E. *Org. Electron.* **2005**, *6*, 11.
(28) Li, N.; Lassiter, B. E.; Lunt, R. R.; Wei, G.; Forrest, S. R. *Appl. Phys. Lett.* **2009**, *94*, 023307.
(29) (a) Perez, M. D.; Borek, C.; Forrest, S. R.; Thompson, M. E. *J. Am. Chem. Soc.* **2009**, *131*, 9281. (b) Schlenker, C. W.; Thompson, M. E. *Chem. Commun.* **2011**, *47*, 3702.
(30) (a) Riedel, I.; Parisi, J.; Dyakonov, V.; Lusten, L.; Vanderzande, D.; Hummelen, J. C. *Adv. Funct. Mater.* **2004**, *14*, 38. (b) Rand, B. P.; Burk, D. P.; Forrest, S. R. *Phys. Rev. B* **2007**, *75*, 115327.